

RESEARCH PAPER



Short-term tissue permeability actions of dextran sulfate sodium studied in a colon organ culture system

Elisabeth M. Danielsen, Alba De Haro Hernando*, Mohammad Yassin, Karina Rasmussen, Jørgen Olsen , Gert H. Hansen, and E. Michael Danielsen

Department of Cellular and Molecular Medicine, the Panum Institute, Faculty of Health Sciences, University of Copenhagen, Copenhagen, Denmark

ABSTRACT

Dextran sulfate sodium (DSS)-induced colitis is the most commonly used animal model for inflammatory bowel diseases. However, the precise molecular action of DSS, in particular its initial effect on the epithelial tissue permeability, is still poorly understood. In the present work, organ culture of mouse – and pig colon explants were performed for 1–2 h in the presence/absence of 2% DSS together with polar- and lipophilic fluorescent probes. Probe permeability was subsequently assessed by fluorescence microscopy. DSS rapidly increased paracellular permeability of 70-kDa dextran without otherwise affecting the overall epithelial integrity. FITC-conjugated DSS likewise permeated the epithelial barrier and strongly accumulated in nuclei of cells scattered in the lamina propria. By immunolabeling, plasma cells, T cells, macrophages, mast cells, and fibroblasts were identified as possible targets for DSS, indicating that accumulation of the polyanion in nuclei was not confined to a particular type of cell in the lamina propria. In contrast, colonocytes were rarely targeted by DSS, but as visualized by transmission electron microscopy, it induced the formation of vacuole-like structures in the intercellular space between adjacent epithelial cells. Nuclei of various cell types in the lamina propria, including both cells of the innate and adaptive immune system, are novel targets for a rapid action of DSS, and from previous *in vitro* studies, polyanions like DSS are known to disrupt nucleosomes by binding to the histones. We therefore propose that nuclear targeting is one way whereby DSS exerts its inflammatory action as a colitogen in animal models of inflammatory bowel diseases.

ARTICLE HISTORY

Received 24 September 2019
Revised 5 February 2020
Accepted 6 February 2020

KEYWORDS

Permeability barrier; colon organ culture; dextran sulfate sodium (DSS)-induced colitis; inflammatory bowel disease (IBD)

Introduction

Inflammatory bowel diseases (IBD), of which Crohn's disease and ulcerative colitis are the main types, are complex and multifactorial diseases commonly characterized by a chronic dysregulated immune response in the gastrointestinal tract.^{1,2} So far, the etiology of IBD is only partially understood, but the pathogenesis is generally thought to involve an interplay between an altered gut microbiota and an aberrant immune response in a genetically prone individual. Furthermore, disease onset can be precipitated by the presence of environmental triggers, for instance, dietary components and antibiotics.³

With IBD affecting 0.2% or more of the population in Western societies, the morbidity

of the diseases combined with the massive treatment costs has spurred the development of experimental animal models that aim to mimic the pathogenesis occurring in humans.⁴ Ideally, such models should provide knowledge about the key features of IBD both with regard to its initial stages and further progression, ultimately leading to new efficient therapeutic options. Here, the dextran sulfate sodium (DSS) model of inflammation, originally described in 1990,⁵ is the one most frequently applied due to its rapidity, simplicity, reproducibility, and controllability.^{6–9} DSS is a water-soluble, polyanionic sulfated polysaccharide of variable size, but usually, DSS in the range of 40–50 kDa is used in model studies. In most protocols, DSS is added to the drinking water at a concentration of 1–5%, and depending on

CONTACT Michael Danielsen  midan@sund.ku.dk  Department of Cellular and Molecular Medicine, The Panum Institute, Building 18.2.36, Blegdamsvej 3, 2200 Copenhagen N, Denmark

*Present address: Autonomous University of Madrid, Ciudad Universitaria de Cantoblanco 28049 Madrid, Spain.

© 2020 The Author(s). Published with license by Taylor & Francis Group, LLC.

This is an Open Access article distributed under the terms of the Creative Commons Attribution-NonCommercial-NoDerivatives License (<http://creativecommons.org/licenses/by-nc-nd/4.0/>), which permits non-commercial re-use, distribution, and reproduction in any medium, provided the original work is properly cited, and is not altered, transformed, or built upon in any way.

the administration regime, the model can mimic either acute (6–10 days) or chronic (4–5 repeated cycles of 1 week) inflammation. The earliest signs of inflammation appearing by day 1 are primarily changes in expression of tight junction-associated proteins, such as occludin, Zonula occludens-1 (ZO-1) and various claudins, causing leaks in the epithelial barrier, as also observed for human IBD.⁶ These initial effects are modest but are subsequently followed by worsening symptoms, including increased permeability, bleeding, and mortality.⁷ Histologically, DSS-induced colitis is characterized by erosions and ulcers, loss of crypts and a heavy infiltration of neutrophils.⁸ The cell types involved in this process include epithelial cells, T cells, neutrophils, and macrophages.¹⁰ The prevailing view is therefore that DSS mimics IBD primarily through a direct action on the epithelial barrier, thereby enabling antigens derived from the gut luminal microbiota to reach the underlying lamina propria. Subsequently to these events, an inappropriate immunological response leading to widespread inflammation is then initiated.⁶ However, the exact molecular mechanism whereby DSS damages the epithelium in the early stages to initiate inflammation is still poorly understood.

The aim of the present study was to investigate the immediate short-term tissue permeability effects on the colonic epithelium when exposed to the actions of DSS.¹¹ To this end, organ culture of colon explants lends itself as an *in vivo*-like model system enabling direct observations of changes occurring within as short a time period as 1–2 h. In recent works, intestinal organ culture has proved particularly useful for studying paracellular- and transcellular permeability effects of a number of lumenally-acting permeation enhancers, using a variety of polar – and lipophilic fluorescent probes.^{12–16} In the present work, using colon obtained from pig and mouse, we observed that DSS within 1–2 h increased the paracellular permeability of FITC-conjugated dextrans, suggesting a rapid action of DSS on tight junction function between neighboring colonocytes. In addition, and more surprising, FITC-conjugated DSS itself permeated

into the lamina propria and strongly accumulated in nuclei of cells scattered within this mucosal region. Nuclei of several different cell types, including those of both the innate and adaptive immune system, were identified as targets for DSS, whereas colonocytes were rarely affected. From previous, *in vitro* studies dextran sulfate and other polyanions are known to be capable of disrupting nucleosomes by forming complexes with histones,^{17,18} and we propose that this novel action *in vivo* contributes to the overall colitogenic properties of DSS.

Materials and methods

Materials

Dextran sulfate sodium (DSS) (from *Leuconostoc* spp.; MW 40 kDa; # 52423; Lot BCBP6912V (DSS40)) was supplied by Sigma-Aldrich (Copenhagen, Denmark; www.sigmaaldrich.com), Texas Red Dextran (MW 3 kDa, lysine fixable; # D3328; Lot 1910381) (TRD3), Oregon Green Dextran (MW 10 kDa, lysine fixable; # D7171; Lot 1801966) (OGD10), Texas Red Dextran (MW 70 kDa, lysine fixable; # D1864; Lot 1985255) (TRD70), a fixable analog of the FM lipophilic styryl dye FM 1–43 FX (FM; # F35355; Lot 1515548), Alexa-conjugated secondary antibodies (# A11034; Lot 1141875, # A11029; Lot 11789729, # A11032; Lot 3954A), and ProLong antifade reagent with DAPI (# P36931; Lot 1867828) by Thermo Scientific (Roskilde, Denmark; www.thermodanmark.dk), 4 kDa FITC-Dextran sulfate sodium (FITC-DSS4; # FD4; Lot 20693), 10 kDa (FITC-DSS10; # FD10; Lot 20652) and 40 kDa (FITC-DSS40; # FD40) by TdB Consultancy AB (Uppsala, Sweden; www.tdbcons.com), polyclonal antibodies to human IgA; # A0262, IgM; # A091, and a monoclonal antibody to human Ki-67 antigen (MIB-1; # M852) by Agilent Technologies Denmark ApS (Glostrup, Denmark; www.agilent.com), a goat polyclonal antibody to human CD4 (# sc-1140; Lot E2809) and a mouse monoclonal antibody to vimentin (# sc-6260) by Santa Cruz Biotechnology Inc. (Dallas, U.S.A.; www.scbt.com), a mouse monoclonal antibody to human CD63 (# 07681165) by Immunotech Inc. (Marseille, France; www.immunotechlab.com),

and a mouse monoclonal antibody to Toll like receptor 5 (# ab-13876; Lot 134582, TLR5) by Abcam Ltd. (Cambridge, UK; www.abcam.com).

Animals

Animal experimentation in Denmark is subject to ethical evaluation by the Ministry of Justice's Council for Animal Experimentation. Animal experimentation included in this work was performed only by licensed staff at the Department of Experimental Medicine, the Panum Institute, University of Copenhagen, and was covered by license 2012-15-2934-00077 issued to the Dept. of Experimental Medicine. As this study contained no further experimentation with live animals, no specific approval by an ethics committee was required. Post-weaned, female animals were used, and a total number of six mice and four pigs were included in the study. No animals were excluded from subsequent data analysis. Prior to experimentation, the animals were kept in the animal storage facilities with free access to feed and water.

Segments of porcine colon (~10 cm), taken from the middle part of overnight fasted, post-weaned animals, were surgically removed from the anesthetized animals and immediately placed in ice-cold RPMI medium. After excision of the tissue, the pigs were sacrificed by an injection with pentobarbital (1 mg/kg bodyweight; Euthanimal (# 28728); Scanvet, Fredensborg, Denmark (www.scanvet.dk)). The colon from female C57BL/6 mice was quickly excised immediately after sacrifice by cervical dislocation of the animals and placed in ice-cold RPMI medium.

Organ culture of colon explants

Organ culture of porcine- and mouse colon tissue was performed essentially as described previously.¹⁹⁻²¹ Briefly, pieces of colon weighing ~0.1 g were quickly excised with a scalpel and transferred to organ culture dishes to which 1 ml of pre-warmed RPMI medium was added. Control explants and explants exposed to DSS40 (2% (w/v) in the medium) were cultured in parallel. The dishes were placed in an incubator kept at 37°C and cultured for 1–2 h, and the various fluorescent membrane probes (ultrafiltration not

required) were added to the medium at the following concentrations: TRD3, OGD10, and TRD70: 0.25 mg/ml, FITC-DSS4, FITC-DSS10, and FITC-DSS40: 2.5 mg/ml, FM: 20 µg/ml. The explants were cultured in the presence of the fluorescent probes for periods of 1–2 h, and after culture, they were rinsed by carefully flushing them with ~2 ml of fresh RPMI medium using a Pasteur pipette. They were finally immersed in a fixative (for details see below in the microscopic methods) and stored at 4°C.

Fluorescence microscopy

Cultured explants were fixed at 4°C for 2 h or overnight in 4% paraformaldehyde in buffer A (0.1 M sodium phosphate, pH 7.2). Following fixation and a quick rinse by immersion in buffer A for 3 × 5 min, the explants were immersed overnight in 25% sucrose in buffer A before mounting in Tissue-Tek and sectioning (~7 µm thick sections) at –19°C in a Leica CM1850 cryostat. For immunolabeling, the sections were incubated for 1 h at room temperature with antibodies to IgA (diluted 1:25000), IgM (diluted 1:2000), CD4 (diluted 1:100), CD63 (diluted 1:100), Ki-67 (diluted 1:100), TLR5 (diluted 1:100), or vimentin (diluted 1:100), in 50 mM Tris-HCl, 150 mM NaCl, 0.5% ovalbumin, 0.1% gelatin, 0.2% teleostan gelatin, 0.05% Tween 20, pH 7.2 (buffer B), followed by incubation for 1 h at room temperature with Alexa 594-conjugated goat anti-rabbit antibodies (diluted 1:200) in buffer B. Controls with omission of primary antibodies were routinely included in the labeling experiments.

Hematoxylin-eosin (HE) staining of fixed tissue sections was performed according to a standard protocol.²²

All sections were finally mounted in antifade mounting medium with DAPI and examined in a Leica DM 4000B microscope fitted with a Leica DFC495 digital camera. Images were obtained using Leica objectives with the following magnification/numerical aperture: 20x/0.40, 40x/0.65, 63x/0.90, and 100x/1.30. The following filter cubes were used: I3 (band pass filter, excitation 450–490 nm), TX2 (band pass filter, excitation 560/40 nm), and A4 (band pass filter, excitation 360/40 nm).

Transmission electron microscopy

For transmission electron microscopy, cultured colon specimens were fixed in 3% glutaraldehyde (v/v) plus 2% (w/v) paraformaldehyde in buffer A overnight at 4°C. After a rinse in buffer A, the explants were post-fixed in 1% osmium tetroxide in buffer A for 1 h at 4°C, dehydrated in acetone and finally embedded in Epon. Ultrathin sections were cut in a Pharmacia LKB Ultratome III, and stained with 1% (w/v) uranyl acetate in H₂O and lead citrate. All sections were finally examined in a Zeiss EM 900 electron microscope equipped with a Mega View II camera.

Results

No visible short-term effects of DSS40 on gross colon morphology after organ culture

Effects of DSS on intestinal epithelial cells have been studied previously, using cell lines as model system.²³ Like epithelial cell lines, organ culture of intestinal explants is a model system suitable for investigating short-term effects of compounds acting at the luminal surface of the gut. In addition, by comparison to commonly used epithelial cell lines, organ culture offers a more *in vivo*-like setting with a preserved crypt architecture in addition to the numerous cell types present in the mucosa. We have used the organ culture system in many previous studies, and have provided evidence that various viability parameters, such as tissue morphology, membrane trafficking processes (endocytosis and exocytosis) and protein biosynthesis remain functional for the duration of the experiments.^{20,21}

In the present work, colonic explants obtained both from mouse and pig were used. Most of the experiments presented were performed with tissues obtained from both animals (including experiments with FITC-DSS and immunolabeling with IgA, IgM, and CD63), but some of the antibodies used for identification of cell types by immunolabeling (Figures 5 and 6) were reactive with only one of the two species (the CD4- and vimentin antibodies were only reactive with the pig proteins and the TLR5 antibody used was only reactive with the mouse protein).

As shown in Figure 1, the gross morphology of the mucosal – and submucosal layers of both

mouse – and pig colonic tissue was generally well preserved after organ culture for up to 2 h. Thus, well-defined crypts containing numerous goblet cells were abundant, and the luminal epithelium generally appeared intact. In addition, Figure 1 shows that DSS40 at a concentration of 2% had no apparent short-term effects on the overall colon morphology. Small clusters of apically exfoliated epithelial cells were occasionally seen both in control – and DSS-treated explants, but this occurrence most likely reflects an ongoing renewal of the epithelium.

Effects of DSS40 on mucosal permeation of polar- and lipophilic probes

A sensitive and convenient method to study permeation effects of DSS40 is to employ fluorescent polar – and lipophilic probes that enable direct visualization of both paracellular- and transcellular pathways from the gut lumen through the colonic epithelium. Dextrans are water soluble, hydrophilic polysaccharides available in different molecular sizes, and as fluorescent conjugates they are useful polar permeation probes due to their uncommon poly-(α -D-1,6-glucose) linkages, which render them resistant to cleavage by most endogenous cellular glycosidases. As shown in Figure 2, the 10-kDa OGD10 freely permeated the epithelium of control explants and accumulated in a broad zone below the basement membrane of the colonocytes after 1 h of culture. In addition, a weaker and diffuse staining of the lamina propria was detectable. The staining of the explant tissue appeared to be largely extracellular, indicating that OGD10 is not taken up by colonocytes or other cells in the lamina propria, either by endocytosis or leakage through the cell membrane. Permeation through the epithelium therefore most likely occurs via the paracellular pathway between neighboring colonocytes, as also implied by the very faint stripy staining along the lateral sides of the epithelial cells. In contrast, the epithelium of the control explant was largely impermeable to the 70-kDa TRD70, both at the luminal surface as well as in the crypts, demonstrating the ability of the colonic mucosa to discriminate between the two probes. However, in the presence of 2% DSS40, OGD10 and TRD70 both permeated the epithelium and distributed

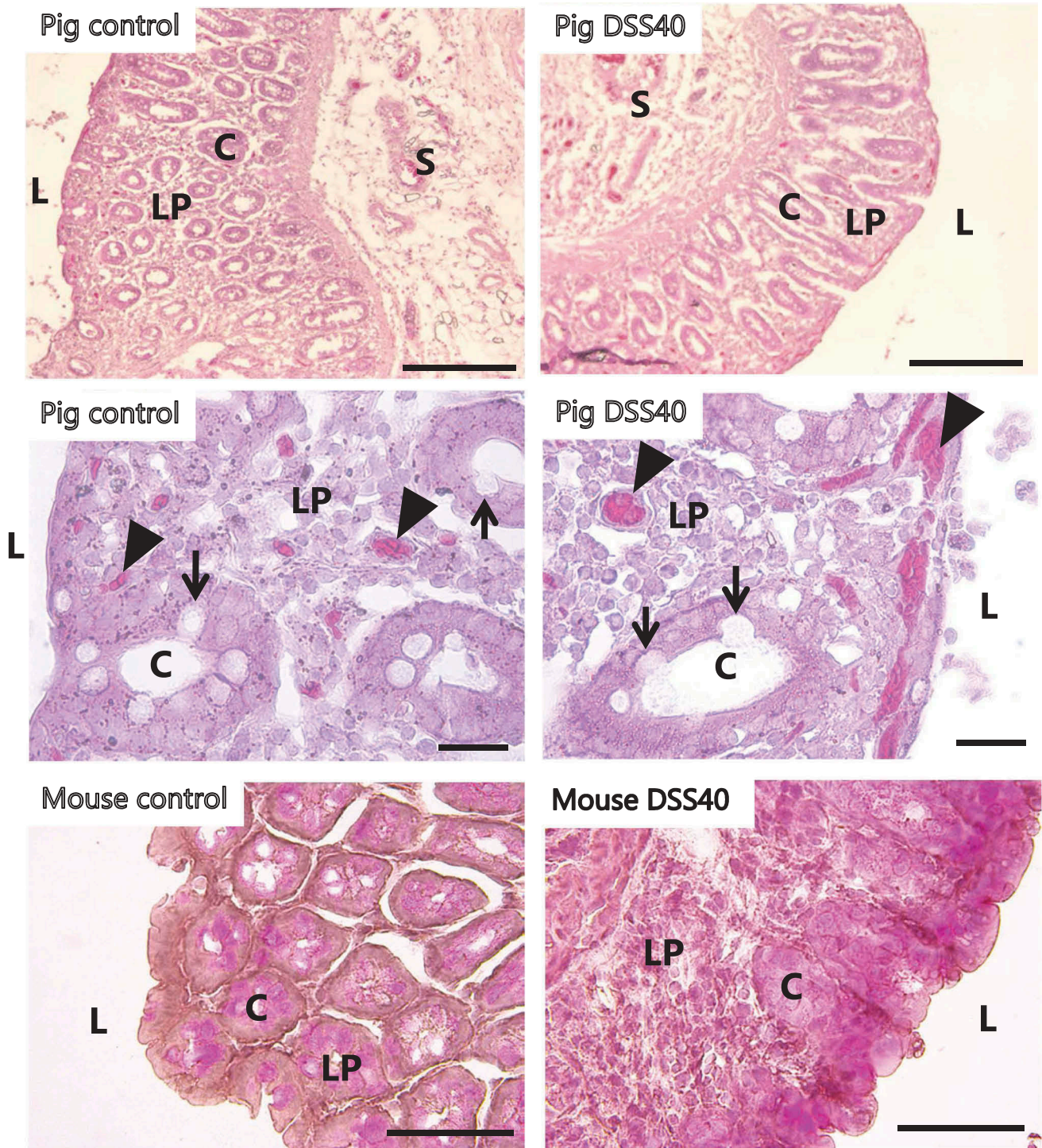


Figure 1. Morphology of colon explants after organ culture. Explants from the colon were cultured for 1 h (mouse) or 2 h (pig) in the absence/presence of 2% DSS40. Representative images of HE-stained sections from both animals showed an overall intact intestinal architecture with well-preserved crypts also in the presence of DSS, and at higher magnification, numerous goblet cells (indicated by arrows) and blood capillaries (indicated by arrowheads) were seen. L; lumen, C; crypt, LP; lamina propria, S; submucosa. (Small differences in the cutting angle of the crypts during cryosectioning make these appear either circular or elongated). Bars: 100 μ m (top images), 20 μ m (middle images), 50 μ m (bottom images).

freely in the lamina propria (Figure 2). As in the control, both probes were confined to the extracellular space, and the stripy staining along the

lateral sides of the colonocytes was more prominent than that seen in the control, implying an increased permeation via the paracellular pathway.

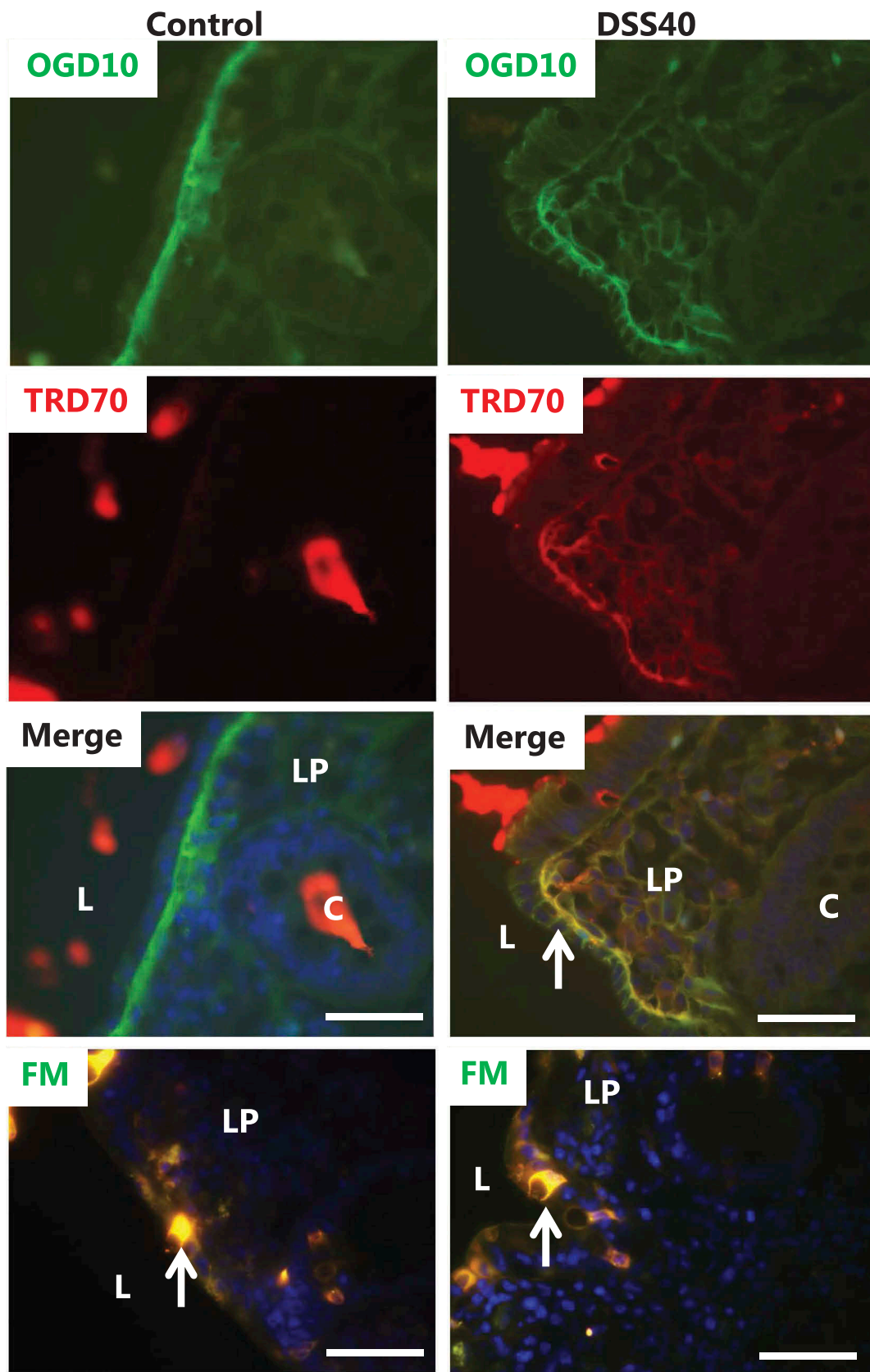


Figure 2. Effect of DSS40 on permeability of polar – and lipophilic probes. Explants from pig colon were cultured for 1 h in the absence/presence of 2% DSS40, and in the presence of both OGD10 and TRD70 or in the presence of FM, as described in Methods. Representative images of cryosections of the labeling profiles of each of the polar probes are shown together with a merged image. L; lumen, C; crypt, LP; lamina propria. Arrows indicate a stripy labeling of the lateral sides of the colonocytes in the merged image of the left panel and goblet cells in the images with FM. Bars: 50 μ m.

FM is a small (MW 560 Da), nontoxic, water-soluble and lipophilic probe that only becomes fluorescent when incorporated into cell membranes, and it has previously been used for uptake studies in the intestinal organ culture system.^{24,25} In control explants, FM intensely labeled the cytosol of goblet cells, as previously observed in the small intestine,²⁵ but it only faintly stained the colonocytes. The lamina propria was largely devoid of staining, indicating that FM is not capable of permeating the epithelium via the paracellular pathway like OGD10. The labeling profile seen in explants treated with 2% DSS40 was similar to that of the control, i.e., strong labeling of the goblet cells, faint staining of the colonocytes and little, if any staining of the lamina propria (Figure 2).

Collectively, the above data show that 1 h of treatment with DSS40 was sufficient to induce detectable changes in the colonic epithelial permeability barrier. The increase in paracellular permeation of the polar probes suggests that the tight junctions between neighboring epithelial cells controlling this pathway are the primary direct site of an immediate DSS40 action. The unchanged low permeability of FM implies that colonocyte cell membrane integrity was not directly affected by DSS during these short-term experiments.

Permeation of FITC-DSS into the colon epithelium

FITC-conjugates of DSS were employed as probes to visualize the distribution and possible sites of action of these polyanionic agents, and Figure 3 shows the labeling profiles of FITC-DSS4, FITC-DSS10 and FITC-DSS40 after 1–2 h of treatment. Most prominently, the probes distinctly labeled the nuclei of cells in the lamina propria, both in mouse- and pig explants. However, not all nuclei of lamina propria cells were thus labeled; the FITC-DSS-positive nuclei were typically located in small or larger clusters, indicating that permeation into the tissue did not occur evenly at the epithelial surface but, more likely, at confined sites. At a much lower level of intensity, diffuse labeling could also be detected in the extracellular space of the lamina propria. In contrast, epithelial cells were rarely labeled, neither in the nuclei nor the cytoplasm. Despite the difference in MW of the three FITC-DSS probes used, no marked size-

dependence in their permeation was observed. Taken together, these results suggest that DSS not only acts to increase permeation of polar compounds, such as dextrans, via the paracellular pathway. Most likely by using this pathway itself, DSS also gains access to the lamina propria and from there is capable of entering cells present in this tissue and to finally accumulate in their nuclei.

The striking difference in tissue distribution of unsubstituted (FITC-TRD3)- and polysulfated (FITC-DSS10) dextrans is demonstrated by the co-labeling experiment shown in Figure 4 where only the latter was localized in the nuclei. Studying the FITC-DSS-positive nuclei in closer detail, they mostly appeared uniformly labeled and of normal globular -or ellipsoid shape. However, highly irregularly shaped nuclei were commonly observed, and in some cases, the labeling was not uniform but mainly confined to the perimeter of the nuclei (Figure 4). These morphological abnormalities suggest that DSS may not merely accumulate passively in the nuclei but act on the nuclear structure.

Identification of mucosal cells permeated by FITC-DSS

A host of different cell types are present in the lamina propria, including various lymphocytes, fibroblasts, eosinophils, and mast cells, in addition to blood capillaries and lymph vessels. To identify which cell types were prone to nuclear targeting by DSS, immunolabeling with antibodies raised to various cell type markers was performed. In these experiments, explants were cultured for 2 h in the presence of FITC-DSS40 to provide a strong nuclear labeling with the probe.

Plasma cells, i.e., B lymphocytes fully differentiated and committed to large-scale synthesis and secretion of various classes of antibodies are amongst the most abundant cells in the intestinal lamina propria.²⁶ As shown in Figure 5, mainly IgA but also IgM secreted from plasma cells diffusively stained extracellular areas of the lamina propria, accumulating both at the basal lamina- and lumen of the crypts. In addition, IgA- and IgM-positive cells were frequently seen scattered in the lamina propria, and cells belonging to both classes in some, but not all cases, had taken up FITC-DSS into their nuclei. However, several cells

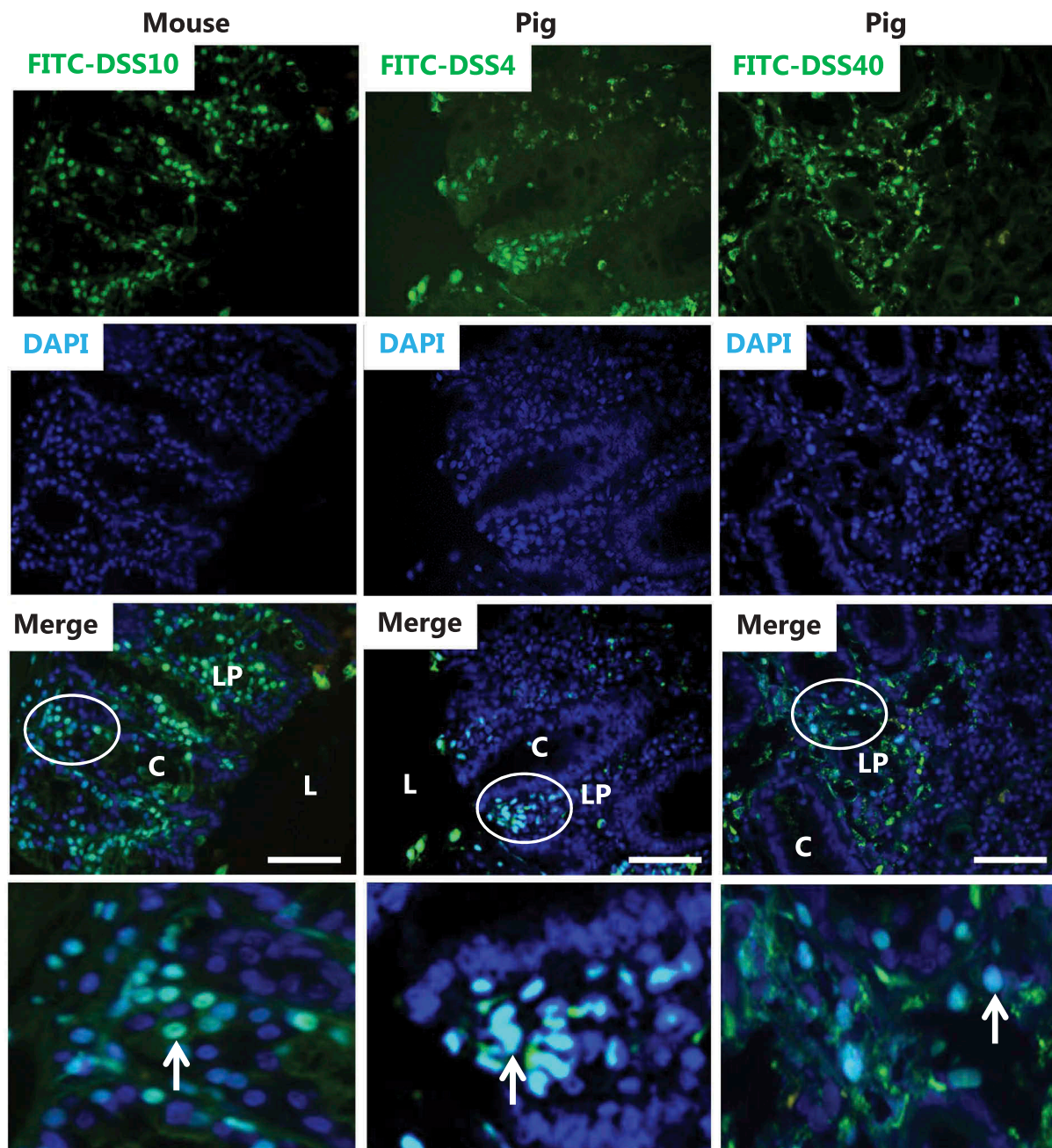


Figure 3. Epithelial permeability and nuclear targeting of FITC-conjugated DSS of various molecular sizes. Images of sections of explants from mouse and pig colon cultured in the presence of FITC-conjugated DSS for 1 h (FITC-DSS4 and FITC-DSS10) or 2 h (FITC-DSS40). Merged images with DAPI staining identify nuclei of cells that have taken up FITC-DSS. L; lumen, C; crypt, LP; lamina propria. The images in the bottom panel show the circled areas in higher magnification. FITC-DSS-positive nuclei (some marked by arrows) of cells are scattered in the lamina propria amongst unaffected cells. Epithelial cells in the crypts were rarely stained by FITC-DSS. Bars: 50 μ m.

in the images shown in [Figure 5](#) with FITC-DSS-positive nuclei were devoid of IgA- or IgM labeling, indicating that plasma cells are not the only cell type targeted by DSS.

Using a similar immunolabeling protocol, the following FITC-DSS-positive cell types were identified in the lamina propria of either mouse – or pig cultured colon explants:

CD4 is a cell surface protein belonging to the immunoglobulin superfamily and functions as a co-receptor of the T cell receptor.²⁷ It is mainly found at the surface of T helper cells and is commonly used as a marker for this cell type, but it is also expressed on monocytes, macrophages, and dendritic cells.²⁸ As shown in [Figure 6](#), nuclei of CD4-positive cells were amongst those targeted by FITC-DSS.

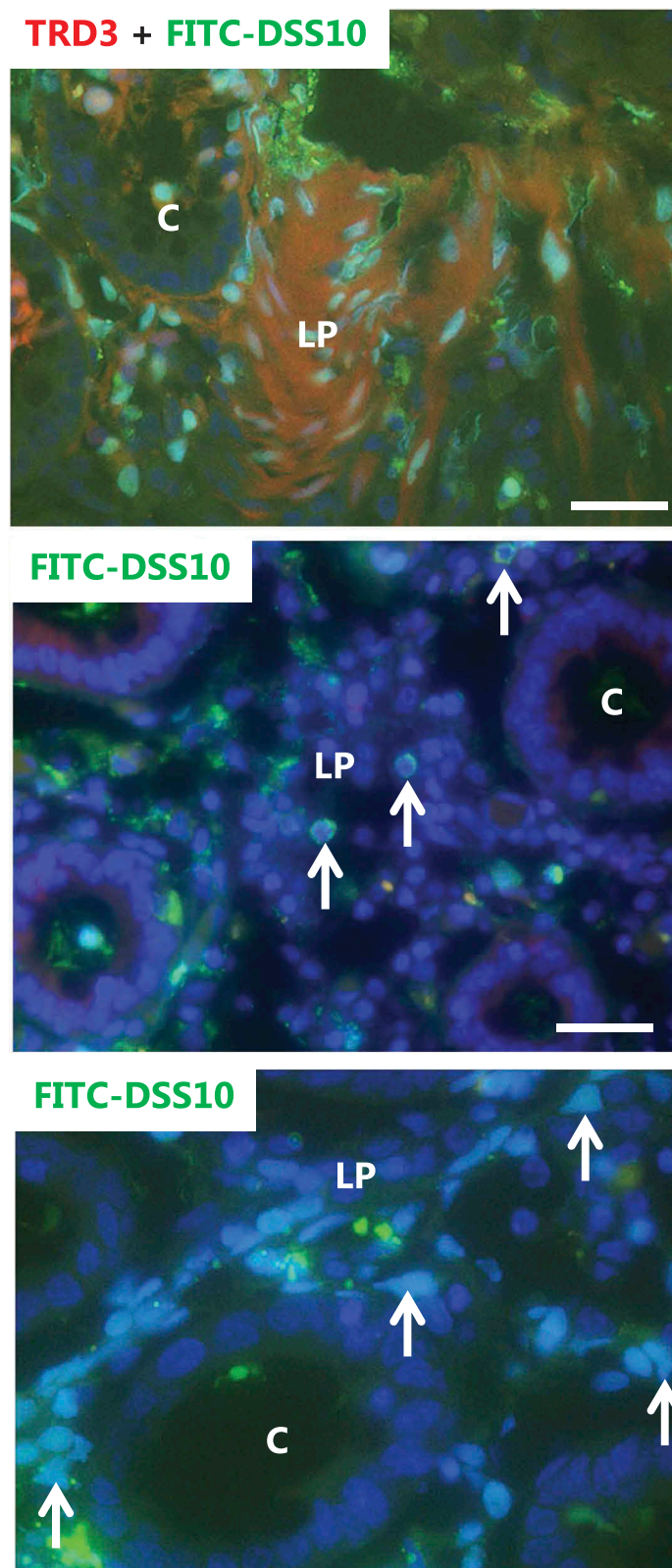


Figure 4. Nuclear targeting of FITC-DSS10, but not of unsubstituted FITC-dextran. Explants from pig colon were cultured for 1 h in the presence of FITC-DSS10 and TRD3. The top image shows that whereas TRD3 mainly stained the lamina propria diffusely, the FITC-DSS10 distinctly targeted nuclei. The nuclei were most often evenly labeled, but occasionally the labeling was confined to the nuclear rim (indicated by arrows in the middle image). The bottom image of increased magnification shows that FITC-DSS10-positive nuclei were sometimes of abnormal shape (indicated by arrows). Bars: 50 μ m.

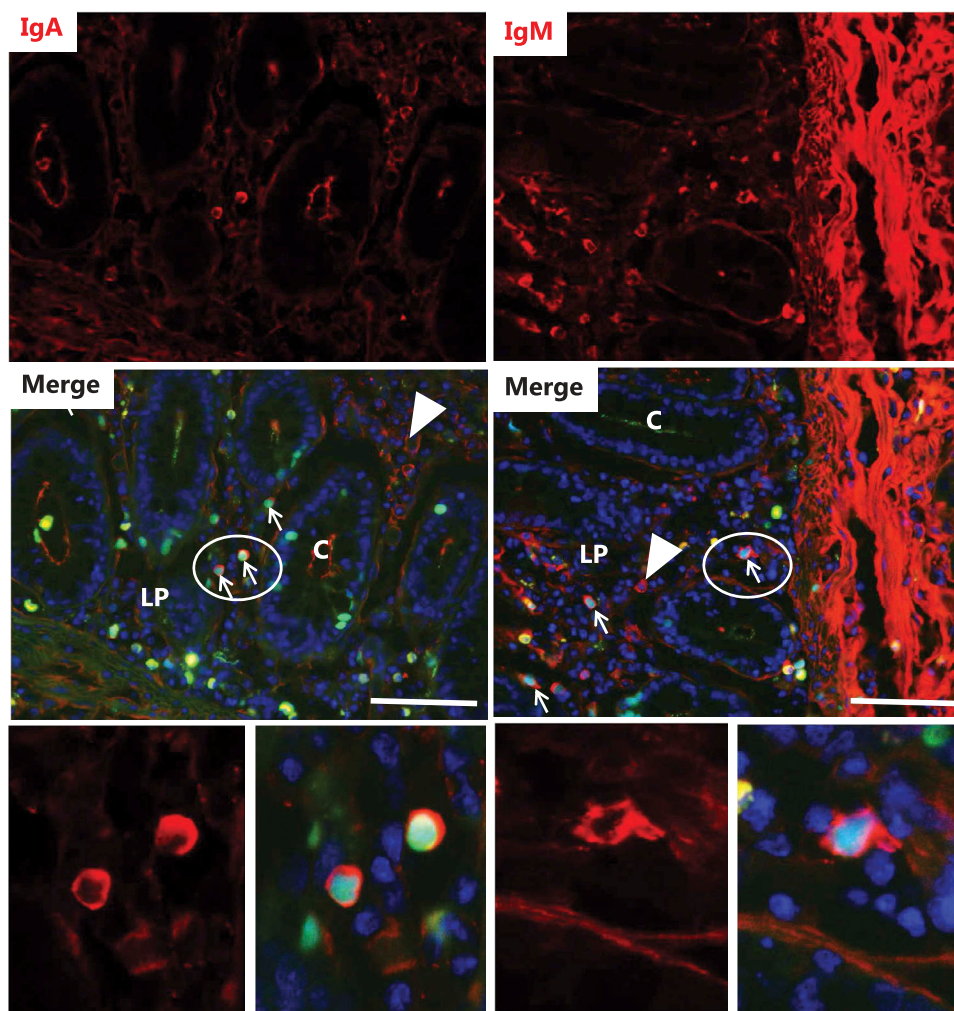


Figure 5. Identification of FITC-DSS40-positive cells I. Explants from pig colon were cultured for 2 h in the presence of FITC-DSS40. Images show sections immunolabeled for IgA or IgM. For both classes of plasma cells, FITC-DSS40-positive nuclei were identified (indicated by arrows), but plasma cells of both classes devoid of the probe were frequently seen as well (indicated by arrowheads). The images in the bottom panel show the circled areas in higher magnification with FITC-DSS40-positive nuclei surrounded by IgA – or IgM labeling in the cytosol. Bars: 50 μm .

CD63, originally discovered on activated platelets, is a member of the tetraspannin family of membrane proteins that are typically found at the cell surface and in secretory granules of basophils and mast cells.²⁹ Figure 6 shows that some of the cells in the lamina propria displaying the characteristic punctate labeling for CD63 in the cytosol also had FITC-DSS-positive nuclei.

Toll-like receptor 5 (TLR5) is a member of a family of cell surface receptors that recognize pathogen-associated molecular patterns (PAMPs). TLR5 is expressed mainly on cells of the innate immune system such as macrophages and dendritic cells but can also be found on T cells.³⁰ Flagellin, a filament protein of bacterial flagella, is the ligand for TLR5 and is

a potent immune activator by initiating a signal cascade that culminates in production of various proinflammatory mediators.³¹ As shown in Figure 6, an antibody to TLR5 distinctly labeled a few cells in the lamina propria, and the nuclei of some but not all of these cells were targeted by DSS.

Vimentin is a widely expressed type III intermediate filament protein but is often used as a marker for fibroblastic cells.^{32,33} Cells in the lamina propria labeled both by the vimentin antibody and FITC-DSS suggest that nuclei of fibroblasts were also susceptible to the action of DSS (Figure 6).

The Ki-67 antigen (recognized by the MIB-1 monoclonal antibody) is a proliferation-related nuclear protein that accumulates in the S phase of the cell cycle

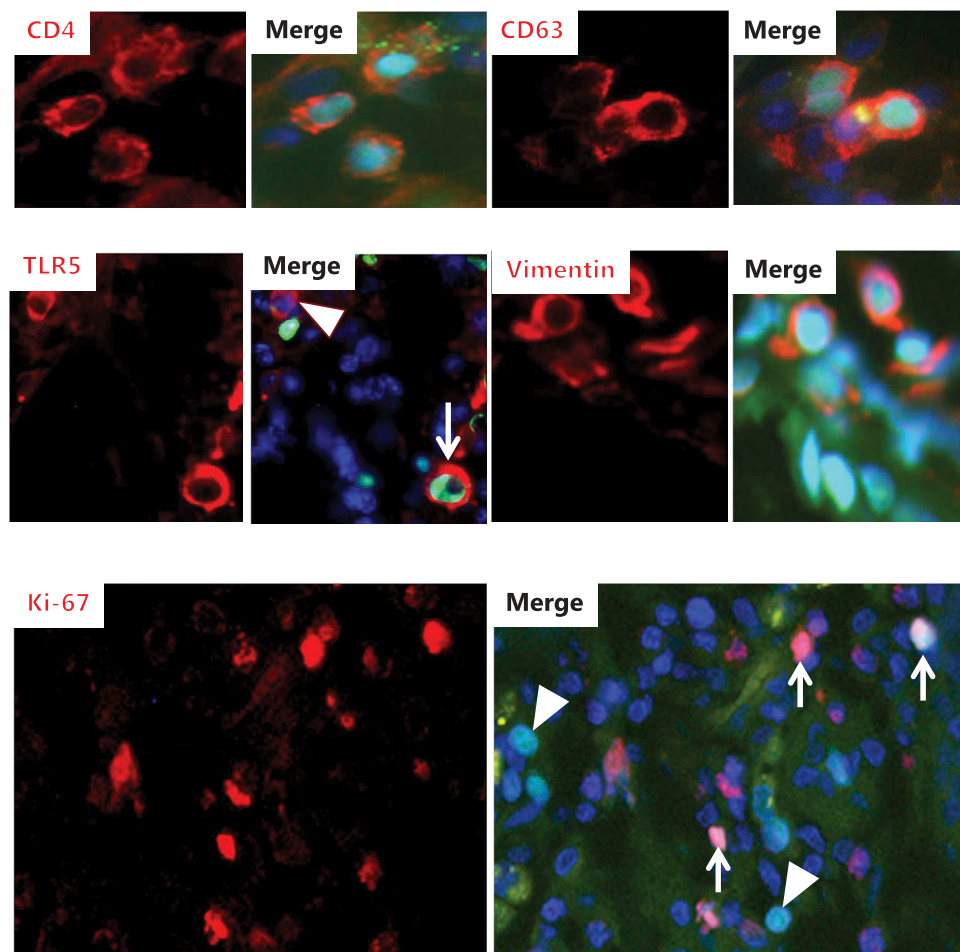


Figure 6. Identification of FITC-DSS40-positive cells II. Explants from pig (CD4, CD63, vimentin, Ki-67) – or mouse (TLR5) colon were cultured for 2 h in the presence of FITC-DSS40. Afterward, sections were immunolabeled with antibodies to CD4, CD63, TLR5, vimentin or Ki-67 (MIB-1). Images of increased magnification show FITC-DSS40-positive nuclei of cells immunolabeled with the respective antibodies. (Arrows indicate cells positive both for FITC-DSS40 and TLR5/Ki-67. Arrowheads indicate a cell positive for TLR5 without FITC-DSS40 and FITC-DSS40-positive cells without labeling for Ki-67.).

and thus is a convenient marker for mitotic cells.^{34,35}

Figure 6 shows that the nuclei of several cells in the lamina propria were prominently labeled by the MIB-1 antibody as well as by FITC-DSS. However, it is also apparent that many FITC-DSS-positive nuclei were devoid of labeling for Ki-67, indicating that nuclear susceptibility to DSS was not restricted to cells undergoing mitosis.

In summary, the above screening for specific cell types as possible targets for nuclear targeting of DSS shows that no single cell type alone was susceptible. Rather, it can be concluded that many cells, including those of both the innate and adaptive immune system present in the lamina propria, are potentially susceptible to this particular action of DSS. In contrast, as indicated by the labeling profiles shown in Figure 2, the epithelial cells did not take up DSS.

Ultrastructure of DSS40-treated mucosal cells

Transmission electron microscopy was employed to study in closer detail any ultrastructural alterations to the epithelium caused by DSS40, and as shown in Figure 7, a striking action of DSS40 was to induce irregularly shaped, vacuole-like structures. On closer inspection, these structures were membrane-enclosed and seemed to be caused by dilation of the normally narrow intercellular space between adjacent colonocytes. Whether some of these vacuoles had become fully engulfed by the epithelial cells, as suggested in some cases by the images, is difficult to ascertain. In contrast, the apical cell surface of colonocytes seemed unaffected by DSS, displaying a normal density of glycocalyx-coated microvilli.

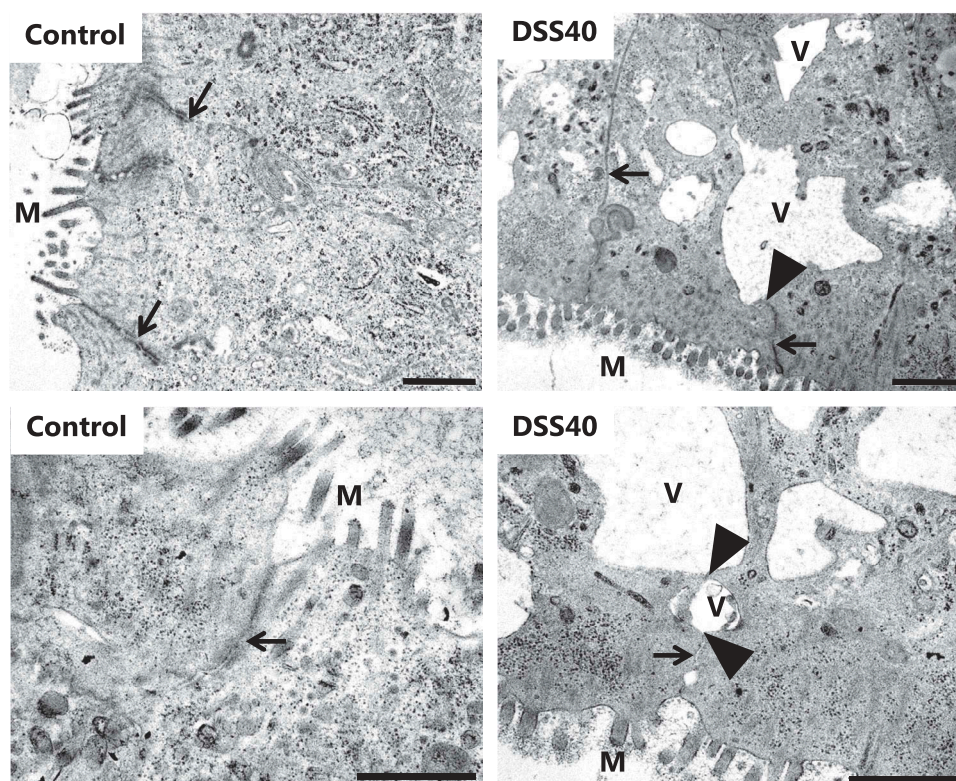


Figure 7. DSS40 action on colon epithelial ultrastructure. Images of ultrathin Epon sections of pig colon explants cultured for 2 h in the absence – or presence of 2% DSS40. The images show the apical part of colonocytes from the crypts with microvilli (m) at the cell surface protruding into the lumen. In the controls, the lateral cell membranes between adjacent colonocytes were always seen in close contact with another (indicated by arrows), but in DSS40-treated explants, the lateral cell membranes frequently separated (indicated by arrowheads), causing the intercellular space to dilate into vacuole-like structures (v). Bars: 1 μ m.

Discussion

The aim of the present work was to investigate possible short-term tissue permeability actions of DSS40 on the colon, and relative to *in vivo* model experiments, which typically run for days, 1 h is a short exposure. Within 1–2 h of treatment in the organ culture system, we identified two targets: 1) the epithelial permeability barrier, and 2) nuclei of a number of different cell types within the lamina propria. In previous studies on the chronological changes induced by DSS administration *in vivo*, early signs of disease (by 1 day) were primarily changes in the expression of tight junction-associated proteins, including occludin, ZO-1, and various claudins.^{6,7–36} For the claudins, early DSS action reportedly included both increased expression of the pore-forming claudin 2 as well as a depletion of sealing claudins (3, 5, 8).³⁷ Only later followed the increasingly worsening of symptoms and histological changes, including mucin depletion, ulceration, and infiltration of granulocytes into the lamina propria

and onset of immune responses.^{6,7} We consider 1–2 h too short a time period to allow for the onset of functional changes in cellular protein expression, implying that the increased paracellular permeability observed in this work most likely was the result of a DSS40 effect on the existing tight junction complexes. A more comprehensive and detailed analysis of the action of DSS on tight junctions would be difficult to undertake with the organ culture system. Nevertheless, the later changes in the expression profiles of proteins controlling the junctional permeability referred to above may well have been initiated by the early action observed in the present work. Thus, as implied by electron microscopy, the increased permeability seemed to be caused by a dilation of the intercellular space along adjacent colonocytes. An osmotic effect of DSS may possibly account for this phenomenon, and it also agrees well with the increased paracellular labeling observed with the polar fluorescent probes OGD10 and TRD70.

The most surprising observation of the present work was the strong accumulation of FITC-DSS in the nuclei of cells, primarily located in the lamina propria. This seemingly specific targeting, to our knowledge not reported previously, was in striking contrast to the diffuse, mainly extracellular distribution seen for the non-sulfated, neutral dextrans, indicating that the polyanionic properties of DSS are the cause of the nuclear accumulation. Along these lines, it is tempting to hypothesize that the driving force for this targeting is an electrostatic interaction with the positively charged DNA-binding histones. This hypothesis lends support from earlier work, where the polyanions dextran sulfate and heparin, when added to chromatin *in vitro*, produced a gel containing a complex of polyanions-histones-DNA, and where subsequent removal of the polyanions resulted in regeneration of nucleosomes.^{17,18} Furthermore, alterations in histone acetylation patterns have previously been associated with IBD in DSS-treated rat models.³⁸ Consequently, the potential ability of DSS to target nuclei and possibly to extract histones from the nucleosomes under *in vivo*-like conditions during a short-term exposure could well be a causative process for the complex scenario of inflammatory reactions that occur at later stages in the development of DSS-induced colitis, in particular as cell types of both the innate- and adaptive immune system were identified. It remains to be clarified by what mechanism FITC-DSS is taken up by its target cells. The absence of any punctate labeling in the cytosol of these cells after 1–2 h of exposure argues against endocytosis of FITC-DSS into early endosomes. Speculatively therefore, a penetration through leaks in the cell membrane, created upon contact with DSS molecules, at present sounds the most likely mechanism.

Conclusion

For almost three decades the DSS animal colitis model of IBD has been employed in numerous basic research studies, and over the years it has provided valuable insight into the complex scenario of events ultimately leading to inflammation after the epithelial barrier has been compromised. We now propose that disruption of the histone-dependent nucleosomal organization of the DNA

in nuclei of cells targeted by DSS should be considered a potential early causative action in the inflammatory response. For instance, DSS itself may exert a direct cytotoxic effect by a nucleosome-disrupting action, leading to cell death and thereby subsequently to the overall activation of the immune system. In a “milder” scenario, nuclear DSS might perturb the normal gene expression profile of affected cells, ultimately triggering an inflammatory response from the immune system. But clearly, further work is needed to elucidate in more detail the consequences of this novel, nuclear action of DSS.

Disclosure of potential conflicts of interest

No potential conflicts to disclose.

Funding

Alba de Haro Hernando was the recipient of an Erasmus traveling grant from the E.U. The study was supported by a grant from Læge Sophus Carl Emil Friis og hustru Olga Doris Friis' Legat.

ORCID

Jørgen Olsen  <http://orcid.org/0000-0003-1974-6446>

References

1. Xavier RJ, Podolsky DK. Unravelling the pathogenesis of inflammatory bowel disease. *Nature*. 2007;448:427–434. doi:10.1038/nature06005.
2. Baumgart DC, Carding SR. Inflammatory bowel disease: cause and immunobiology. *Lancet*. 2007;369:1627–1640. doi:10.1016/S0140-6736(07)60750-8.
3. Ananthakrishnan AN, Bernstein CN, Iliopoulos D, Macpherson A, Neurath MF, Ali RAR, Vavricka SR, Fiocchi C. Environmental triggers in IBD: a review of progress and evidence. *Nat Rev Gastroenterol Hepatol*. 2018;15:39–49. doi:10.1038/nrgastro.2017.136.
4. Cohen RD, Yu AP, Wu EQ, Xie J, Mulani PM, Chao J. Systematic review: the costs of ulcerative colitis in Western countries. *Aliment Pharmacol Ther*. 2010;31:693–707. doi:10.1111/j.1365-2036.2010.04234.x.
5. Okayasu I, Hatakeyama S, Yamada M, Ohkusa T, Inagaki Y, Nakaya R. A novel method in the induction of reliable experimental acute and chronic ulcerative colitis in mice. *Gastroenterology*. 1990;98:694–702. doi:10.1016/0016-5085(90)90290-H.

6. Eichele DD, Kharbanda KK. Dextran sodium sulfate colitis murine model: an indispensable tool for advancing our understanding of inflammatory bowel diseases pathogenesis. *World J Gastroenterol*. 2017;23:6016–6029. doi:10.3748/wjg.v23.i33.6016.
7. Chassaing B, Aitken JD, Malleshappa M, Vijay-Kumar M. Dextran sulfate sodium (DSS)-induced colitis in mice. *Curr Protoc Immunol*. 2014;104. Unit. doi:10.1002/0471142735.2014.104.issue-1.
8. Kiesler P, Fuss IJ, Strober W. Experimental models of inflammatory bowel diseases. *Cell Mol Gastroenterol Hepatol*. 2015;1:154–170.
9. Randhawa PK, Singh K, Singh N, Jaggi AS. A review on chemical-induced inflammatory bowel disease models in rodents. *Korean J Physiol Pharmacol*. 2014;18:279–288. doi:10.4196/kjpp.2014.18.4.279.
10. Gkouskou KK, Deligianni C, Tsatsanis C, Eliopoulos AG. The gut microbiota in mouse models of inflammatory bowel disease. *Front Cell Infect Microbiol*. 2014;4:28. doi:10.3389/fcimb.2014.00028.
11. Bak A, Ashford M, Brayden DJ. Local delivery of macromolecules to treat diseases associated with the colon. *Adv Drug Deliv Rev*. 2018;136–137:2–27. doi:10.1016/j.addr.2018.10.009.
12. Danielsen ET, Danielsen EM. Glycol chitosan: A stabilizer of lipid rafts in the intestinal brush border. *Biochim Biophys Acta*. 2017;1859:360–367. doi:10.1016/j.bbamem.2016.12.017.
13. Danielsen EM, Hansen GH. Probing the action of permeation enhancers sodium cholate and N-dodecyl-beta-D-maltoside in a porcine jejunal mucosal explant system. *Pharmaceutics*. 2018;10:172.
14. Danielsen EM, Hansen GH. Probing paracellular - versus transcellular tissue barrier permeability using a gut mucosal explant culture system. *Tissue Barriers*. 2019;7:1601955. doi:10.1080/21688370.2019.1601955.
15. Danielsen EM, Hansen GH. Impact of cell-penetrating peptides (CPPs) melittin and Hiv-1 Tat on the enterocyte brush border using a mucosal explant system. *Biochim Biophys Acta*. 2018;1860:1589–1599. doi:10.1016/j.bbamem.2018.05.015.
16. Danielsen EM, Hansen GH. Intestinal surfactant permeation enhancers and their interaction with enterocyte cell membranes in a mucosal explant system. *Tissue Barriers*. 2017;5:e1361900. doi:10.1080/21688370.2017.1361900.
17. Prusov AN, Fais D, Polyakov VY. Formation of compact globular particles in interphase nuclei from rat liver under the effect of polyanions. *Biochem Biophys Res Commun*. 1993;193:591–598. doi:10.1006/bbrc.1993.1665.
18. Nakashima A, Mori K, Sasaki S. Interaction between polyanions and cell nuclei: mechanism of gelatination of nuclei. *Biochem Biophys Res Commun*. 1996;228:846–851. doi:10.1006/bbrc.1996.1742.
19. Browning TH, Trier JS. Organ culture of mucosal biopsies of human small intestine. *J Clin Invest*. 1969;48:1423–1432. doi:10.1172/JCI106108.
20. Danielsen EM, Sjoström H, Noren O. Biosynthesis of intestinal microvillar proteins. Characterization of intestinal explants in organ culture and evidence for the existence of pro-forms of the microvillar enzymes. *Biochem J*. 1982;202:647–654.
21. Lorenzen US, Hansen GH, Danielsen EM. Organ culture as a model system for studies on enterotoxin interactions with the intestinal epithelium. *Methods Mol Biol*. 2016;1396:159–166.
22. Wittekind D. Traditional staining for routine diagnostic pathology including the role of tannic acid 1. Value and limitations of the hematoxylin-eosin stain. *Biotech Histochem*. 2003;78:261–270. doi:10.1080/10520290310001633725.
23. Ni J, Chen SF, Hollander D. Effects of dextran sulphate sodium on intestinal epithelial cells and intestinal lymphocytes. *Gut*. 1996;39:234–241. doi:10.1136/gut.39.2.234.
24. Bolte S, Talbot C, Boutte Y, Catrice O, Read ND, Satiat-Jeuemaitre B. FM-dyes as experimental probes for dissecting vesicle trafficking in living plant cells. *J Microsc*. 2004;214:159–173. doi:10.1111/j.0022-2720.2004.01348.x.
25. Hansen GH, Rasmussen K, Niels-Christiansen -L-L, Danielsen EM. Endocytic trafficking from the small intestinal brush border probed with FM dye. *Am J Physiol Gastrointest Liver Physiol*. 2009;297:G708–G715. doi:10.1152/ajpgi.00192.2009.
26. Neutra MR, Mantis NJ, Kraehenbuhl JP. Collaboration of epithelial cells with organized mucosal lymphoid tissues. *Nat Immunol*. 2001;2:1004–1009. doi:10.1038/ni1101-1004.
27. Biddison WE, Shaw S. CD4 expression and function in HLA class II-specific T cells. *Immunol Rev*. 1989;109:5–15. doi:10.1111/j.1600-065X.1989.tb00017.x.
28. McDougal JS. Function of the CD4 molecule in normal immune responses. *Curr Opin Immunol*. 1988;1:88–91. doi:10.1016/0952-7915(88)90057-X.
29. Koberle M, Kaesler S, Kempf W, Wölbing F, Biedermann T. Tetraspanins in mast cells. *Front Immunol*. 2012;3:106. doi:10.3389/fimmu.2012.00106.
30. Kabelitz D. Expression and function of Toll-like receptors in T lymphocytes. *Curr Opin Immunol*. 2007;19:39–45. doi:10.1016/j.coi.2006.11.007.
31. Honko AN, Mizel SB. Effects of flagellin on innate and adaptive immunity. *Immunol Res*. 2005;33:83–101. doi:10.1385/IR:33:1.
32. Fuchs E, Weber K. Intermediate filaments: structure, dynamics, function, and disease. *Annu Rev Biochem*. 1994;63:345–382. doi:10.1146/annurev.bi.63.070194.002021.
33. Tarbit E, Singh I, Peart JN, Rose-Meyer RB. Biomarkers for the identification of cardiac fibroblast and myofibroblast cells. *Heart Fail Rev*. 2019;24:1–15. doi:10.1007/s10741-018-9720-1.
34. Schonk DM, Kuijpers HJ, van DE, van Dalen CH, Geurts van Kessel AHM, Verheijen R, Ramaekers FCS. Assignment of the gene(s) involved

- in the expression of the proliferation-related Ki-67 antigen to human chromosome 10. *Hum Genet.* 1989;83:297–299. doi:10.1007/BF00285178.
35. Bruno S, Darzynkiewicz Z. Cell cycle dependent expression and stability of the nuclear protein detected by Ki-67 antibody in HL-60 cells. *Cell Prolif.* 1992;25:31–40. doi:10.1111/j.1365-2184.1992.tb01435.x.
 36. Poritz LS, Garver KI, Green C, Fitzpatrick L, Ruggiero F, Koltun WA. Loss of the tight junction protein ZO-1 in dextran sulfate sodium induced colitis. *J Surg Res.* 2007;140:12–19. doi:10.1016/j.jss.2006.07.050.
 37. Yuan B, Zhou S, Lu Y, Liu J, Jin X, Wan H, Wang F. Changes in the expression and distribution of claudins, increased epithelial apoptosis, and a mannan-binding lectin-associated immune response lead to barrier dysfunction in dextran sodium sulfate-induced rat colitis. *Gut Liver.* 2015;9:734–740. doi:10.5009/gnl14155.
 38. Tsaprouni LG, Ito K, Powell JJ, Adcock IM, Pouchard N. Differential patterns of histone acetylation in inflammatory bowel diseases. *J Inflamm (Lond).* 2011;8:1. doi:10.1186/1476-9255-8-1.